

## **4.2 *Multilateration methods***

1. Target location and tracking
2. Range-Doppler plots
3. Ghosts
4. Parameter estimation
5. Doppler method
6. Circular arrays

# Target location and tracking

A passive bistatic radar system can measure :

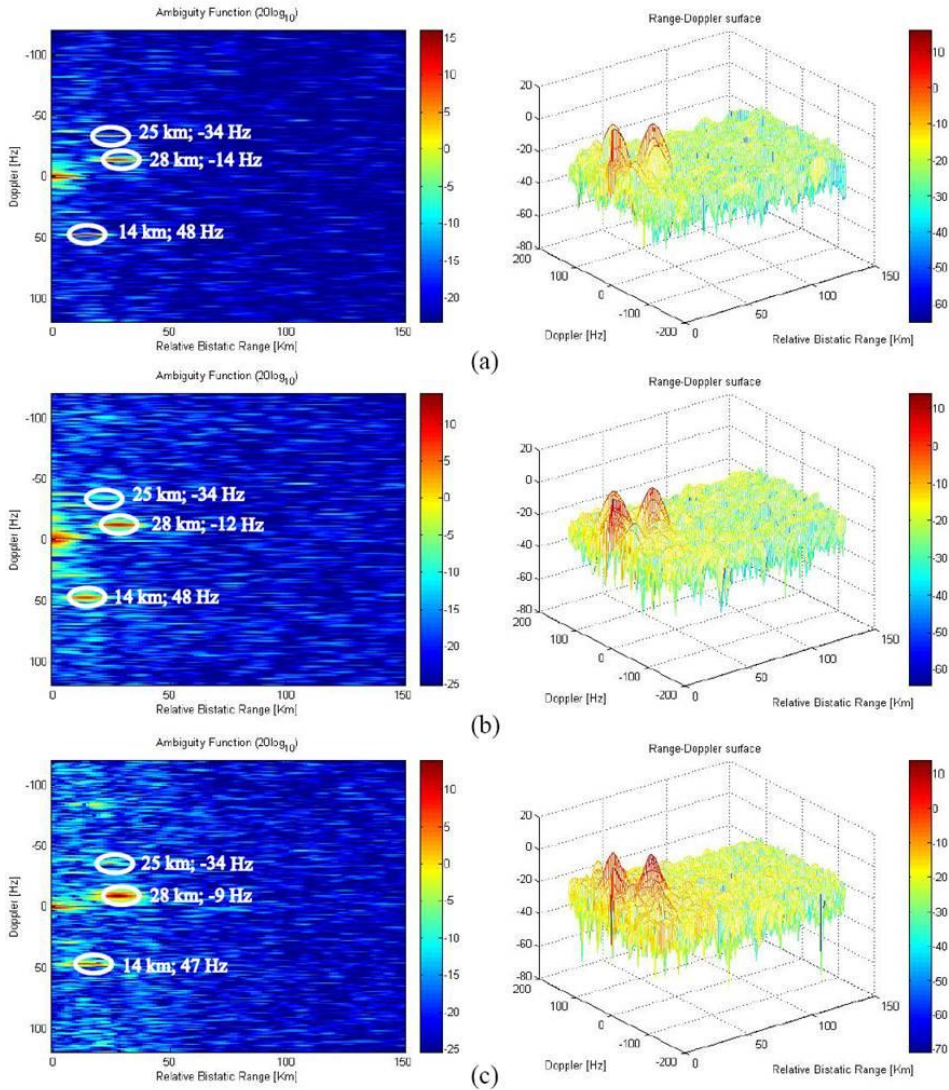
- bistatic range (from delay difference between direct signal and echo)
- echo Doppler
- echo angle of arrival

from one or more transmissions

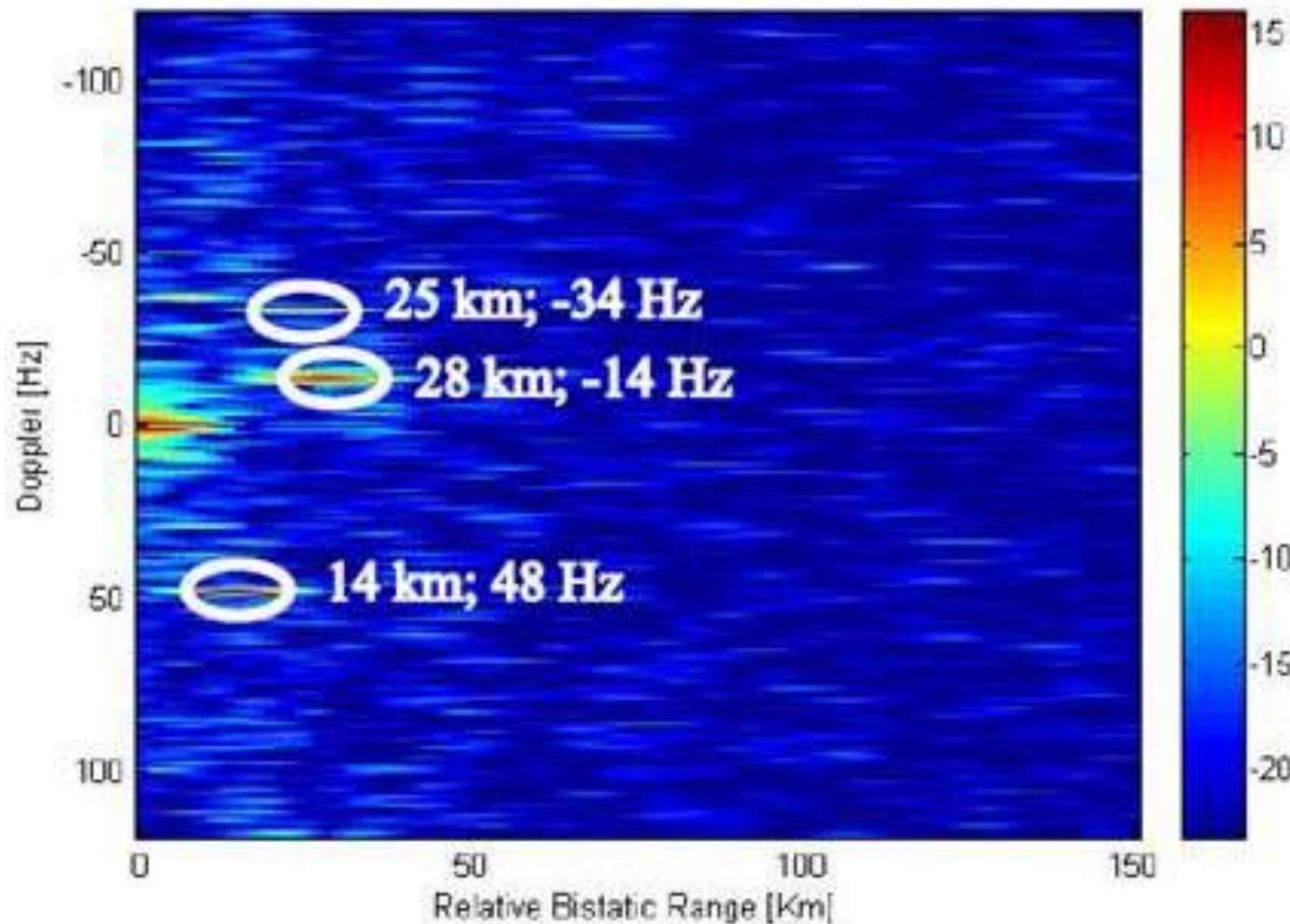
How can such measurements be combined to locate and track targets ?

- multilateration
- parameter estimation

# Range-Doppler plots



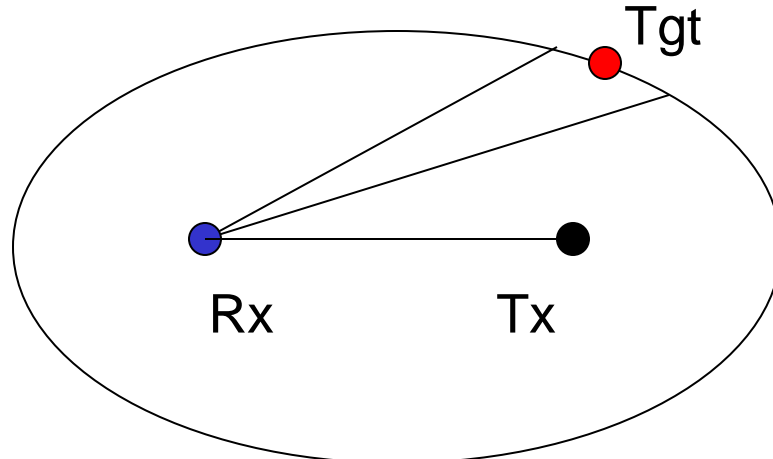
# Range-Doppler plots



# Bistatic vs multistatic target state estimation – for location

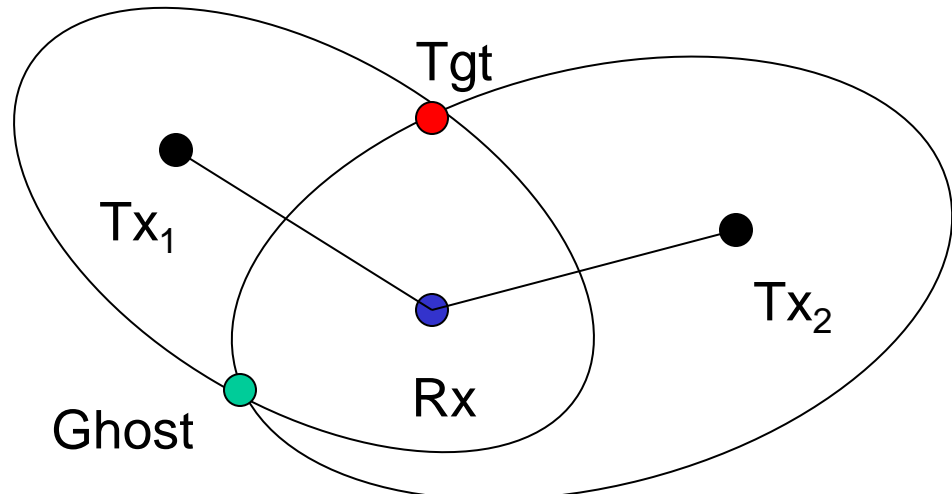
TYPICAL BISTATIC:

Baseline  
Range sum  
Receive look angle

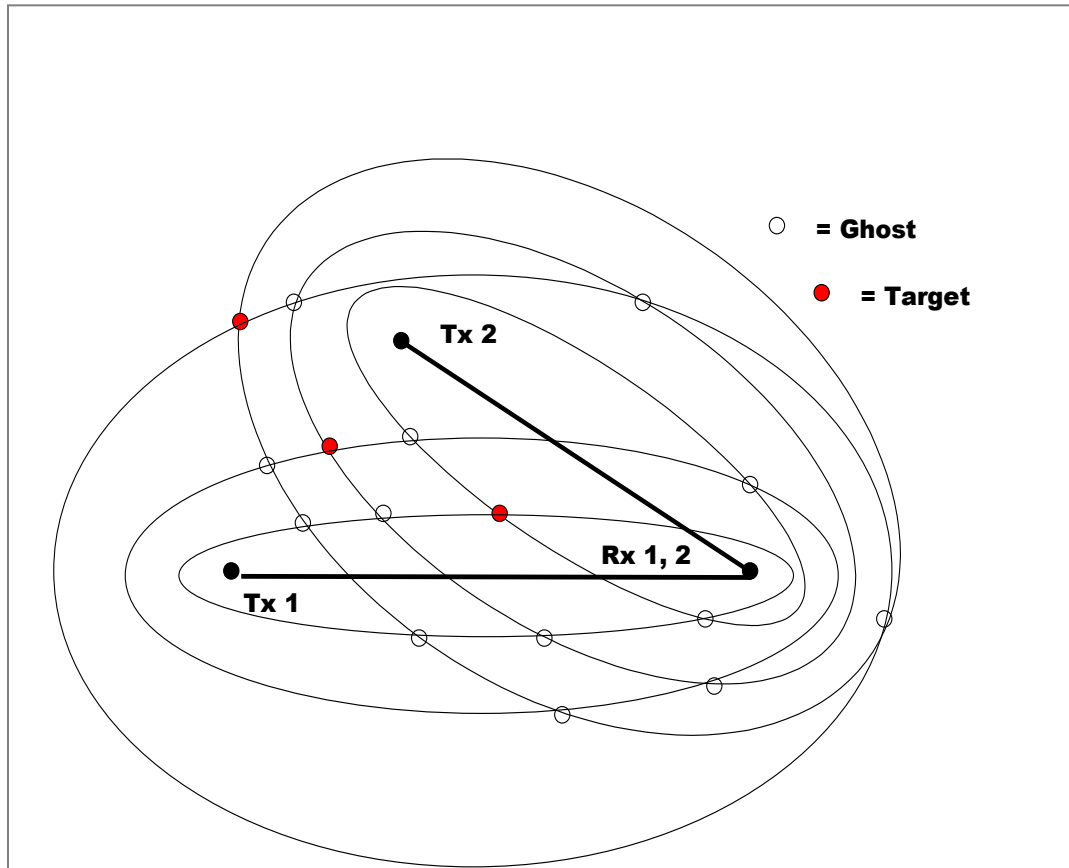


TYPICAL  
MULTISTATIC:

Baseline  
Two range sums



# Caspers' ghosts



Jim Caspers was author of the Bistatic Radar chapter in Skolnik's first Radar Handbook. He worried about ghosts generated by bistatic multilateration systems. And we must still worry about them causing spurious detections and tracks whenever the system does not generate adequate spatial resolution via antenna directivity. Using more Tx – Rx links with overlapping coverage---when available---as an alternative solution. Silent Sentry now uses this approach.

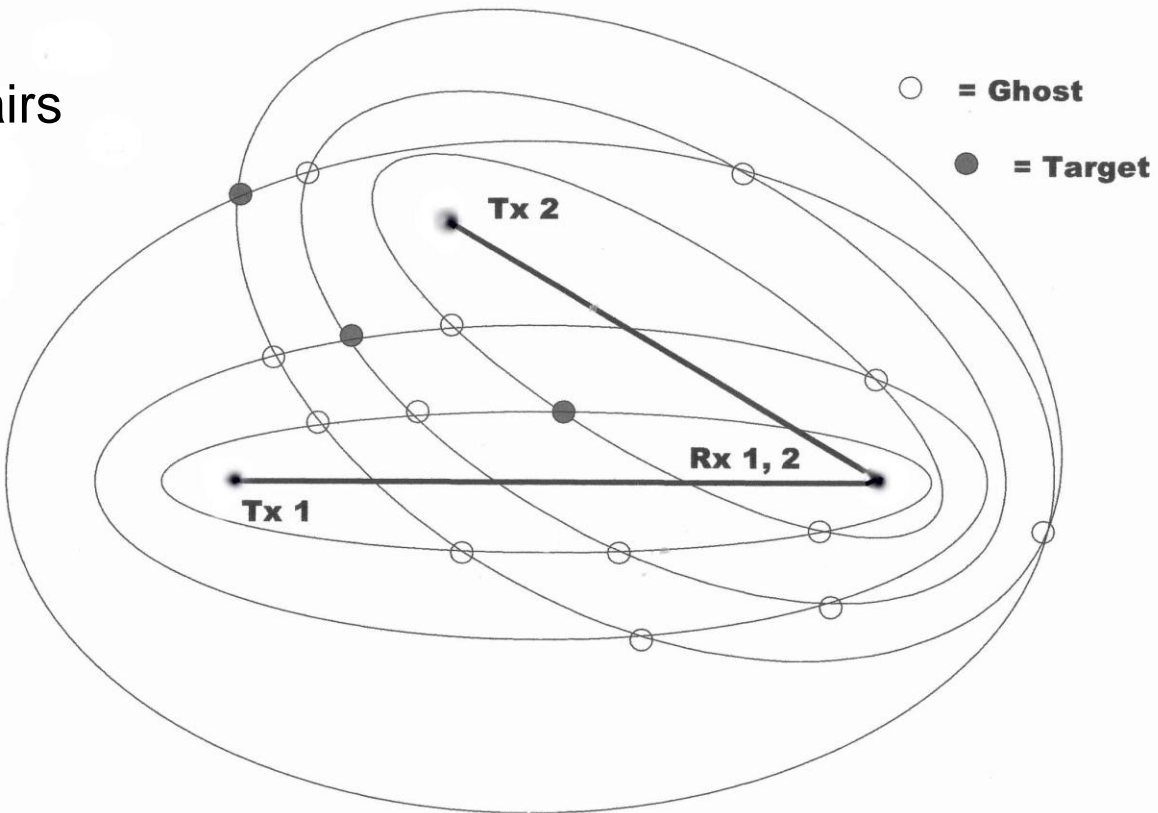
# But more targets: more ghosts

$$\# \text{ ghosts} = (2n^2 - n) (N^2 - N)/2$$

where:  $n = \# \text{ targets}$   
 $N = \# \text{ Tx/Rx pairs}$

Example:

$$n = 3, N = 2$$
  
 $\# \text{ ghosts} = 15$



# Until it gets really ugly

courtesy of Paul Howland's NATO test bed

**KEY:**

Rx: 0,0

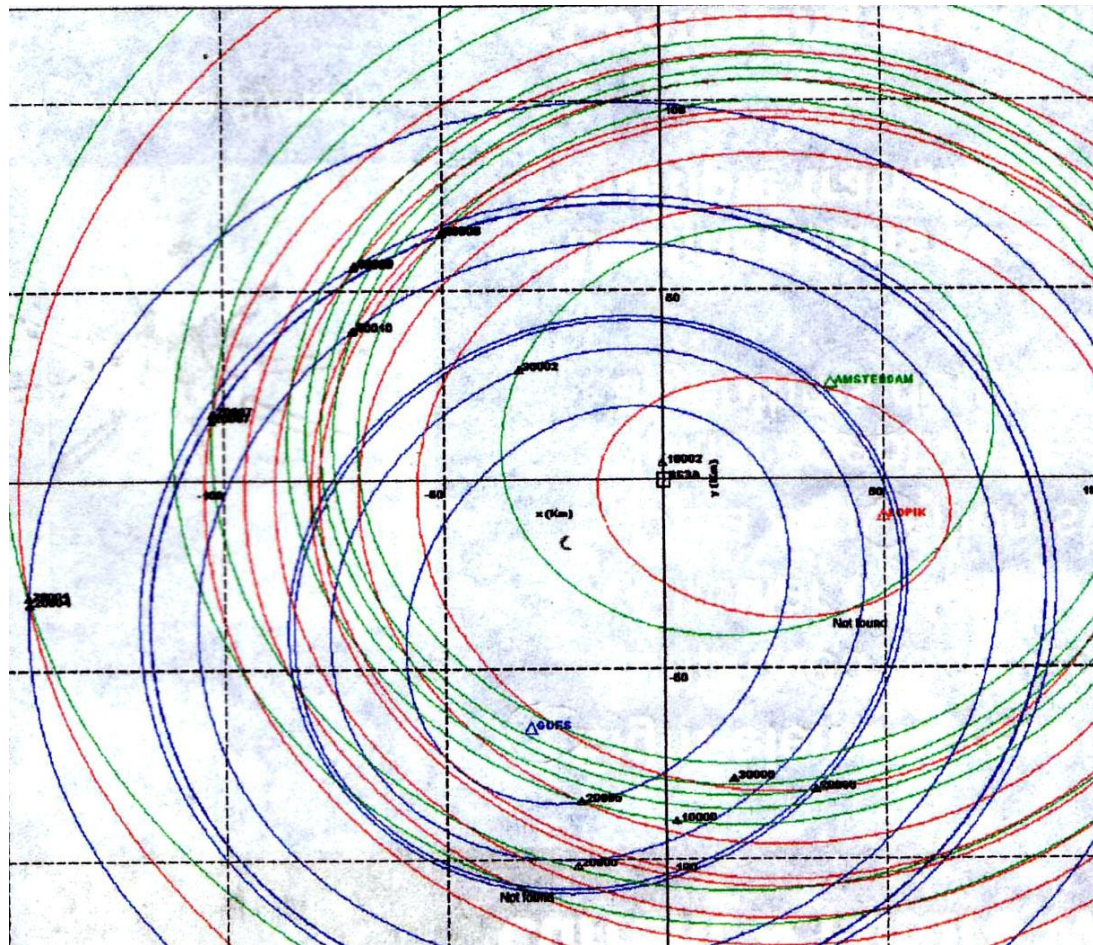
Tx: 3 (Red, blue, green)

Tgts: 9

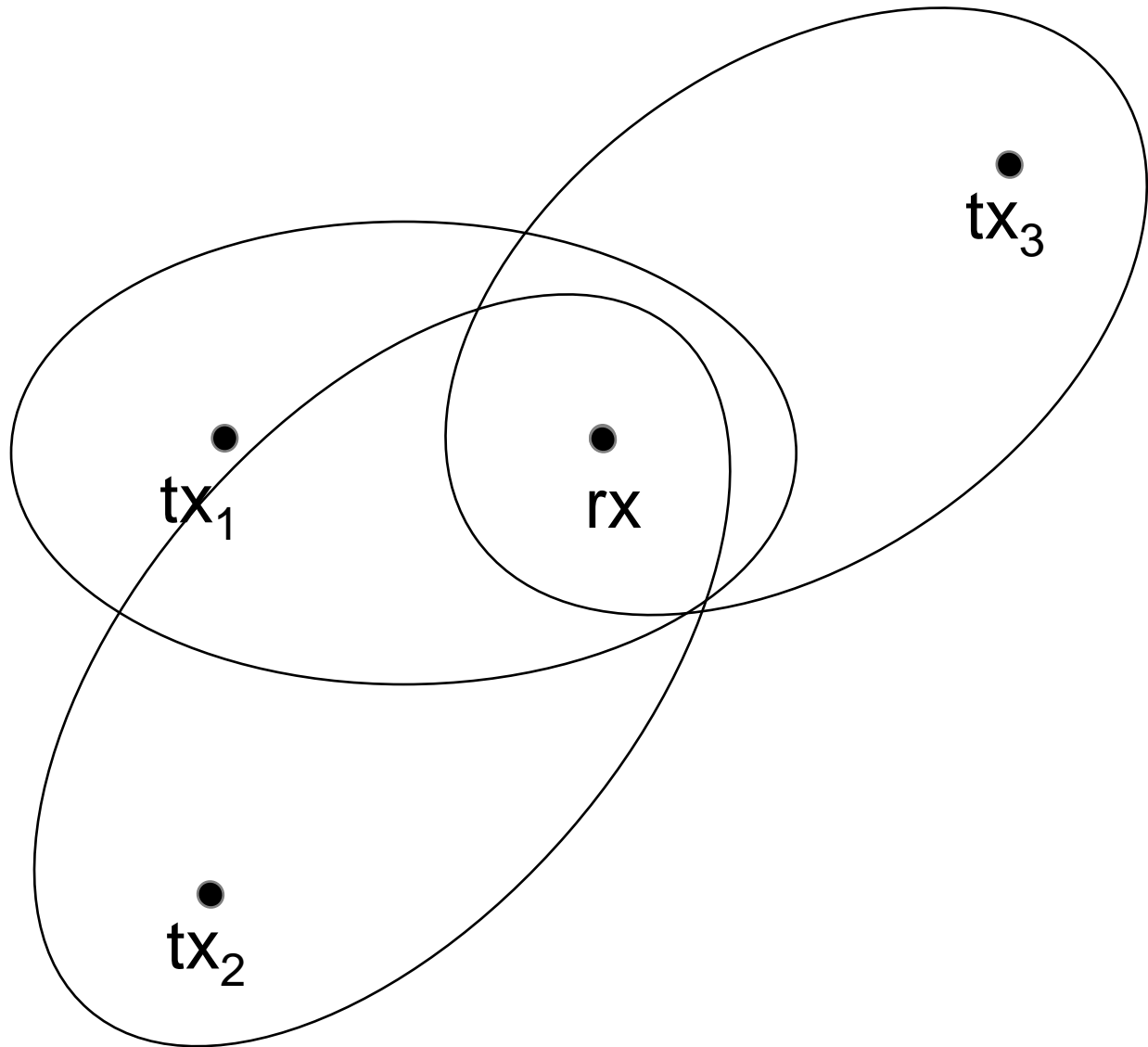
True tgts: Located by  
ATC radars

Ghosts: All other  
intersections

**AND THEY MUST BE  
EXCISED**



# Multilateration



# Parameter estimation

Set up a target state vector, and use sequence of measurements to give best estimates of vector components.

Similar approach to classical tracking theory.

L. G. deBay, 'Tracking in Space by DOPLOC', *IRE Trans. on Military Electronics*, pp332-335, April-July 1960.

Howland, P. E., 'Target tracking using television-based bistatic radar', *IEE Proc. Radar Sonar and Navigation*, Vol. 146, No.3, June 1999, pp166-174.

Howland, P.E., Maksimiuk, D. and Reitsma, G., 'FM radio based bistatic radar', Special Issue of *IEE Proc. Radar, Sonar and Navigation* on Passive Radar Systems, Vol.152, No.3, pp107–115, June 2005.

# Parameter estimation

Suppose that the receiver is located at the origin of a Cartesian coordinate system with the transmitter at  $(0, L)$ . A target is located at  $(x_0, y_0)$  at time  $t_0$  and is moving with velocity components  $(\dot{x}, \dot{y})$ . If the radar derives the Doppler spectrum at intervals of  $T$  seconds, then after  $n$  samples at time  $t = (t_0 + nT)$  the Doppler shift and bearing of the target are

$$F(n) = \frac{1}{\lambda} \left[ \frac{(x_0 + nT\dot{x})\dot{x} + (y_0 + nT\dot{y})\dot{y}}{\sqrt{(x_0 + nT\dot{x})^2 + (y_0 + nT\dot{y})^2}} + \frac{(x_0 + nT\dot{x})\dot{x} + [L - (y_0 + nT\dot{y})]\dot{y}}{\sqrt{(x_0 + nT\dot{x})^2 + (y_0 + nT\dot{y})^2}} \right]$$

and

$$\theta(n) = \tan^{-1} \left( \frac{x_0 - nT\dot{x}}{y_0 - nT\dot{y}} \right)$$

P.E. Howland, H.D. Griffiths and C.J. Baker, 'Passive Bistatic Radar', chapter in *Bistatic Radar: Emerging Technology* (M. Cherniakov ed.), Wiley, 2008.

Howland, P. E., 'Target tracking using television-based bistatic radar', *IET Proc. Radar Sonar and Navigation*, Vol. 146, No.3, June 1999, pp166-174. June 2005.

# Parameter estimation

The measurements of Doppler are therefore functions of the known parameters  $n$ ,  $T$ ,  $L$  and  $\lambda$ , and the unknown track parameters  $(x_0, \dot{x}, y_0, \dot{y})$ .

The unknown track parameters can be estimated from a sequence of measurements of Doppler  $F_m(k)$  and DOA  $\theta_m(k)$  for samples at times  $k = 0, \dots, (m - 1)$  by a straightforward minimization process.

Consider a vector of measurements

$$z^T = (F_m(0), \theta_m(0), F_m(1), \theta_m(1), \dots, F_m(m - 1), \theta_m(m - 1))$$

and a corresponding vector of state equations

$$h^T(x) = (F(0), \theta(0), F(1), \theta(1), \dots, F(m - 1), \theta(m - 1))$$

# Parameter estimation

The problem is then one of attempting to minimize the least square difference between the measurements and the state equations by selecting the best values of the track parameters,  $x$ . The difference is defined as:

$$J_{LS} = \frac{1}{2} [z - h(x)]^T [z - h(x)]$$

This can be minimized by any of a number of standard algorithms, including steepest descent, Gauss-Newton and Levenberg-Marquardt. In order for these to work properly, the least squares difference  $J_{LS}$  should have a unique and well-defined minimum.

Because the information contained in individual measurements of Doppler and direction of arrival is low, relatively long integration periods, of the order of a minute in practice, are found to be necessary. In addition, a good initial estimate of the target state is required.

# Parameter estimation

A more efficient approach, once the track has become established, is to use a Kalman filter. Because the measurements of Doppler and direction of arrival are related to the target track in a very nonlinear fashion, a nonlinear version of the Kalman filter, such as the Extended Kalman Filter (EKF), Unscented Kalman Filter (UKF) or Particle Filter (PF) will be appropriate.

The EKF estimates the target state from the Doppler and angle of arrival measurements as follows:

$$\widehat{x}(t_n) = x(t_n) + K(t_n)y(t_n) - h(x(t_n), t_n)$$

where  $y(t_n)$  is the vector of Doppler and DOA measurements at time  $t_n$ ,  $h(x(t_n), t_n)$  is the measurement that would be expected at time  $t_n$  given the predicted state  $x(t_n)$ , and  $K(t_n)$  is the Kalman gain at time  $t_n$ .

# Parameter estimation

These are calculated from:

$$x(t_n) = f(\hat{x}(t_{n-1}), t_n)$$

predicted track state at time  $t_n$  given its state at time  $t_{n-1}$

$$\mathbf{K}(t_n) = \mathbf{P}_x^-(t_n) \mathbf{M}^T(t_n) [\mathbf{M}(t_n) \mathbf{P}_x^-(t_n) \mathbf{M}^T(t_n) + \mathbf{P}_v(t_n)]^{-1}$$

Kalman gain

# Parameter estimation

where

$$\mathbf{P}_x^{\prime}(t_n) = \Phi(t_n) \mathbf{P}_x(t_{n-1}) \Phi^T(t_n) + \mathbf{G}$$

covariance of the state prediction  $x(t_n)$

$$\mathbf{P}_x(t_{n-1}) = \mathbf{I} - \mathbf{K}(t_{n-1}) \mathbf{M}(t_{n-1}) \mathbf{P}_x^{\prime}(t_{n-1})$$

covariance of the previous smoothed estimate,  $\hat{x}(t_{n-1})$

$$\mathbf{M}(t_n) = \frac{\partial \mathbf{h}(x(t_n), t_n)}{\partial x}$$

linearized measurement matrix

$$\Phi(t_n) = \frac{\partial f(\hat{x}(t_n), t_n)}{\partial x}$$

linearized state equations

and  $\mathbf{P}_v(t_n)$  is the covariance matrix representing the measurement errors  
and  $\mathbf{G}$  is a covariance matrix representing errors in the state equations.

# Parameter estimation

The measurement vector is defined as where  $F$  and  $\theta$  represent the measurements of Doppler and DOA respectively:

$$F = -\frac{1}{\lambda} \left[ \frac{xx'Y - yy'Y}{\sqrt{x^2 + y^2}} + \frac{yy'Y + (L - y)y'y}{\sqrt{x^2 + (L - y)^2}} \right]$$

$$\theta = \tan^{-1} \left( \frac{y}{x} \right)$$

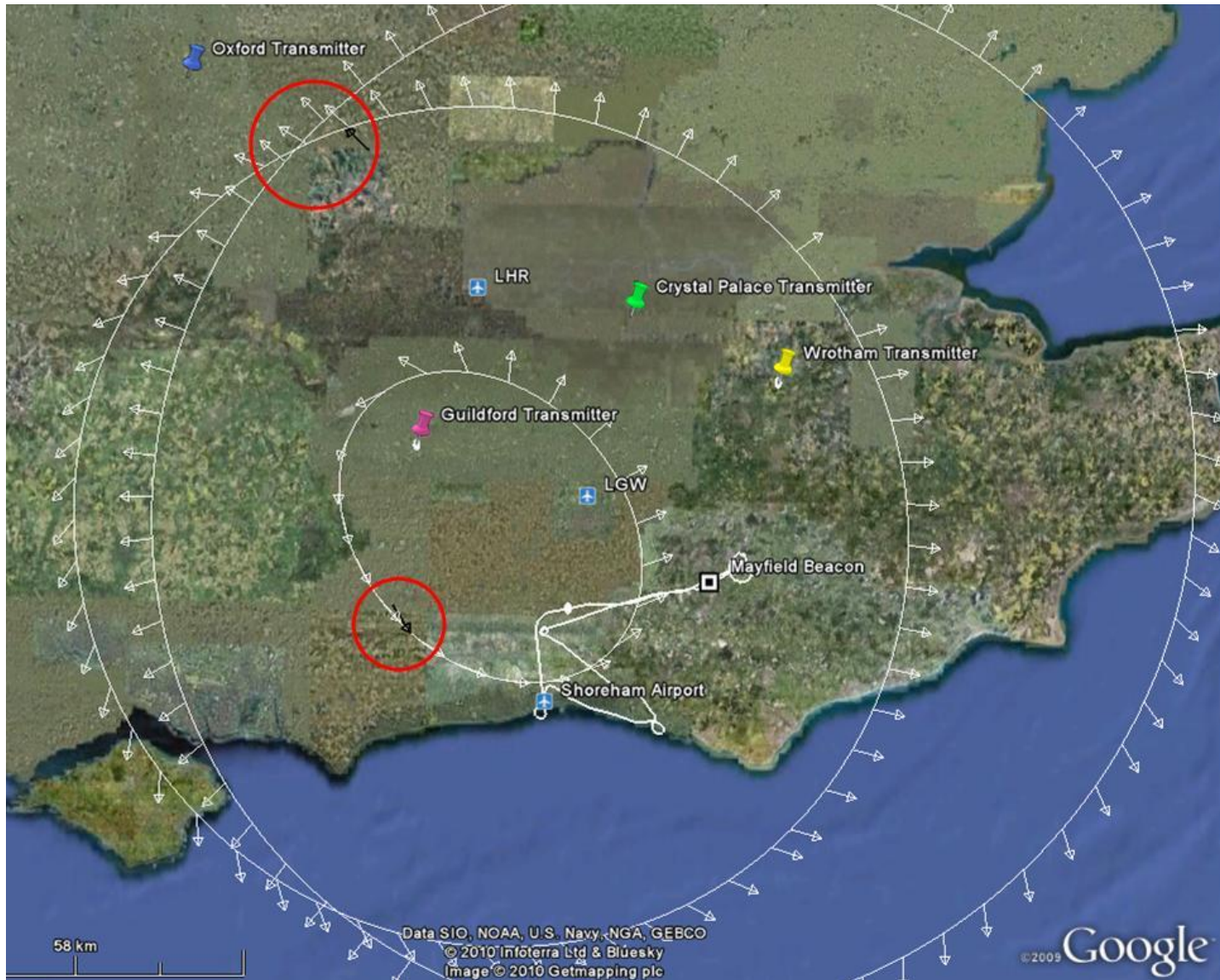
and, assuming a simple linear model for target motion, the state equations are defined as:

$$f(\hat{x}(t_n), t_n) = \begin{pmatrix} x(t_{n-1}) + x'Y(t_{n-1})\Delta t \\ y(t_{n-1}) + y'Y(t_{n-1})\Delta t \end{pmatrix}$$

# PBR with an aircraft-borne receiver

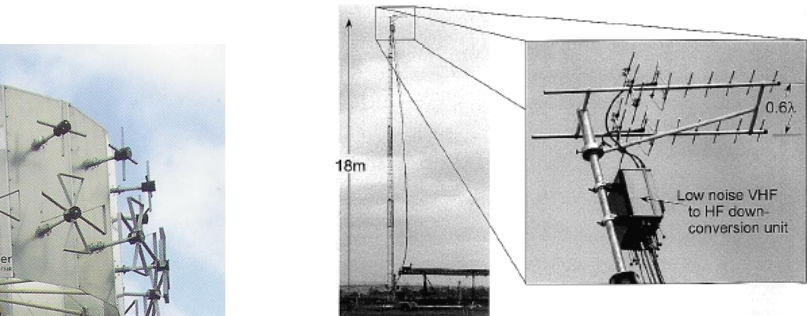


# PBR with an aircraft-borne receiver



# Circular arrays

Many practical PBR systems use circular antenna arrays:

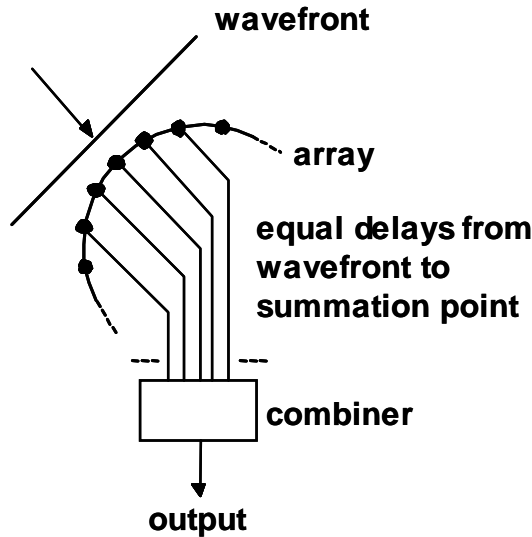


# Beam cophasal excitation

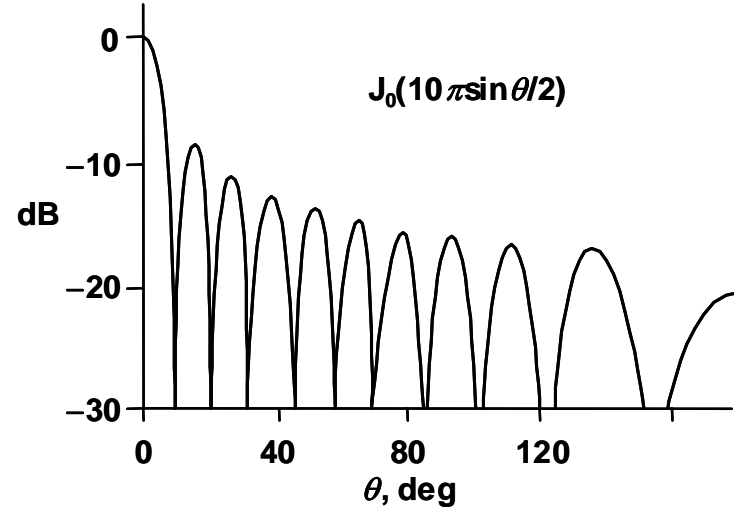
The simplest method of feeding a circular array is simply to arrange for the signals from all the elements to add coherently in the particular direction of interest. For omnidirectional elements, and assuming that the number of elements is large, this gives an azimuth-plane beam of the form

$$D(\theta) = J_0\left(\frac{4\pi}{\lambda} \sin \frac{\theta}{2}\right)$$

(a)



(b)



# Phase mode excitation

Consider firstly a continuous circular array (i.e. one with an infinite number of elements and negligible interelement spacing), and suppose that the elements are omnidirectional. The excitation of the array  $F$  can be regarded as a periodic function of azimuth angle  $\theta$ , of period  $2\pi$ , and can therefore be expressed as a Fourier series

$$F(\theta) = \sum_{m=-N}^N C_m \exp(jm\theta)$$

Each term of the series is known as a *phase mode*, and the coefficient  $C_m$  (which is in general complex) is a *phase mode coefficient*. It can be seen that the zero-order phase mode ( $m=0$ ) corresponds to an excitation of constant phase as a function of azimuth angle.

The first-order phase mode ( $m = 1$ ) corresponds to one cycle of phase over  $360^\circ$  of azimuth; the second-order phase mode ( $m = 2$ ) corresponds to two cycles of phase over  $360^\circ$  of azimuth, and so on. The negative-order phase modes simply correspond to phase variation in the opposite sense.

# Phase modes – far field

When an array is excited by a single phase mode, the far-field pattern  $D_m(\theta)$  has a similar form

$$\begin{aligned} D_m(\theta) &= C_m j^m J_m(\beta r) \exp(jm\theta) \\ &= K_m \exp(jm\theta) \end{aligned}$$

where  $J_m(\cdot)$  is the Bessel function of order  $m$ ,  $\beta = 2\pi/\lambda$ , and  $r$  is the array radius.

# Phase modes – far field

The far-field phase modes are omnidirectional in azimuth, but each with the same characteristic variation of phase with azimuth angle as the corresponding excitation phase mode.

The frequency-dependence of this expression is contained in the Bessel function, so for omnidirectional elements the variation of the phase mode amplitudes with frequency follows the Bessel function.

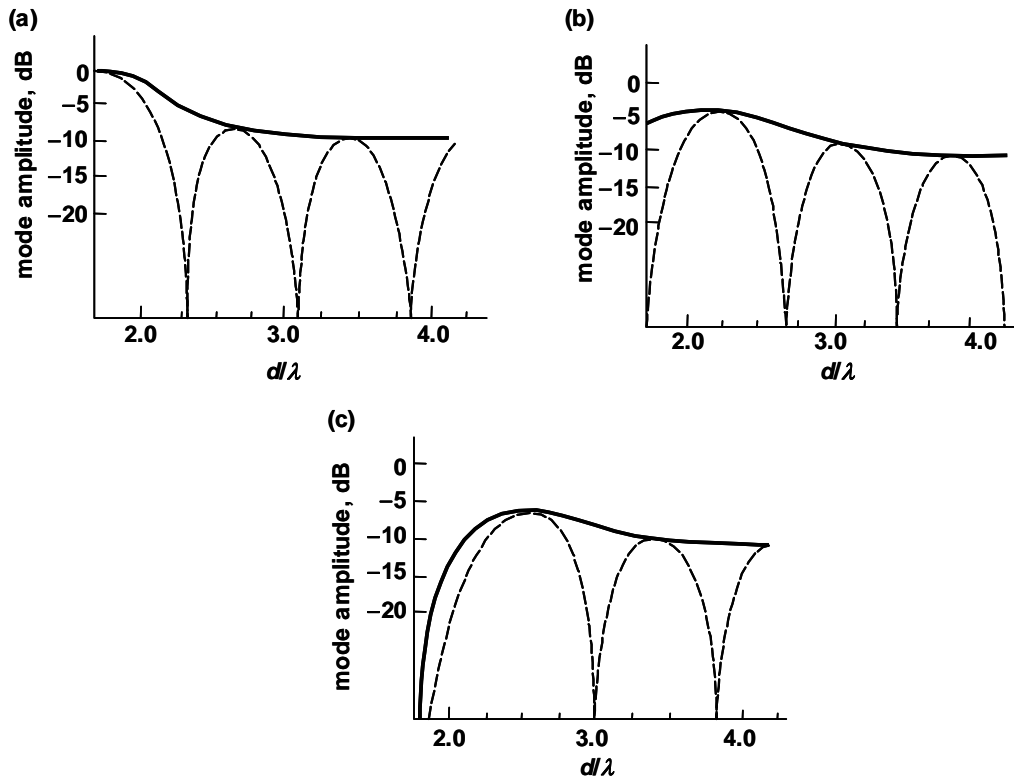
For directional elements the corresponding expression is no longer a single Bessel coefficient, but a series of terms, each corresponding to the Fourier coefficients of the element pattern.

For the particular case of an element pattern of the form  $(1 + \cos\theta)$ , which is a reasonable approximation to many practical elements, the equivalent expression is

$$D_m(\phi) = C_m j^m [J_m(\beta r) - j J'_m(\beta r)] \exp(jm\theta)$$

# Phase modes – far field

This gives a much flatter variation of phase mode amplitude with frequency, since the maxima of  $J_m(\beta r)$  correspond to the zeroes of  $J_m'(\beta r)$  (and vice versa), which is much more suitable for broadband operation.



Calculated variation of phase mode amplitude with frequency: (a) zero-order mode; (b) first-order mode; (c) second-order mode: ----- omnidirectional elements; ———  $(1 + \cos q)$  directional element patterns.

# Discrete array

When a discrete array is used exactly the same theory applies, but the excitation function  $F(\theta)$  is sampled at the element locations by a sampling function  $S(\theta)$ . For an array of  $n$  omnidirectional elements

$$S(\theta) = \sum_{q=-\infty}^{\infty} \exp(jnq\theta) = 1 + \sum_{q=1}^{\infty} \exp(jnq\theta) + \sum_{q=-\infty}^{-1} \exp(jnq\theta)$$

giving

$$\begin{aligned} D_m(\theta) &= C_m j^m J_m(\beta r) \exp(jm\theta) \\ &+ \sum_{q=1}^{\infty} C_m j^{-g} J_{-g}(\beta r) \exp(-jg\theta) \\ &+ \sum_{q=-\infty}^{-1} C_m j^h J_h(\beta r) \exp(jh\theta) \end{aligned}$$

where  $g = (nq-m)$  and  $h = (nq+m)$ .

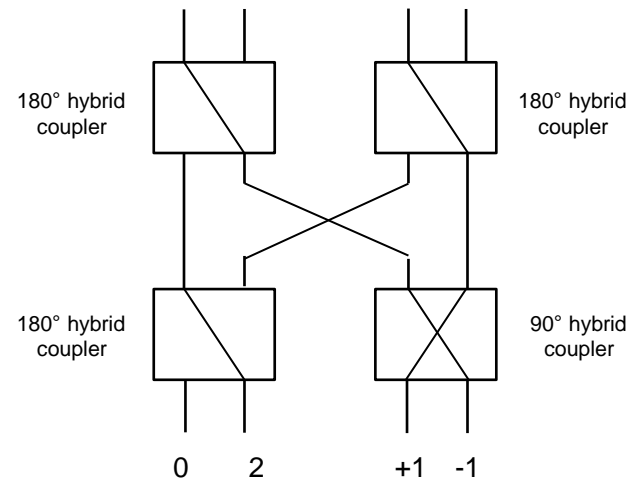
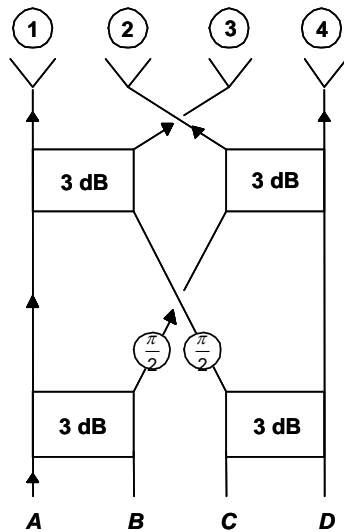
# Discrete array

The first part of this expression is identical to that for a continuous array. The two series represent ripple terms as a function of  $\theta$  (spatial ripple). As a rule of thumb, to keep the spatial ripple acceptably low, the interelement spacing should be no greater than  $\lambda/2$ , which in practice provides an upper limit to the frequency of operation.

For an  $n$ -element array it is possible to generate  $n+1$  phase modes, though the  $+n/2$  and  $-n/2$  phase modes are actually identical. The discrete Fourier Transform to generate the phase modes from the element signals is conveniently provided by a Butler Matrix. The bandwidth is usually limited to about one octave by that of the quadrature hybrid couplers that form part of the Butler Matrix, though with special-purpose components it is possible to improve upon this.

# Butler matrix

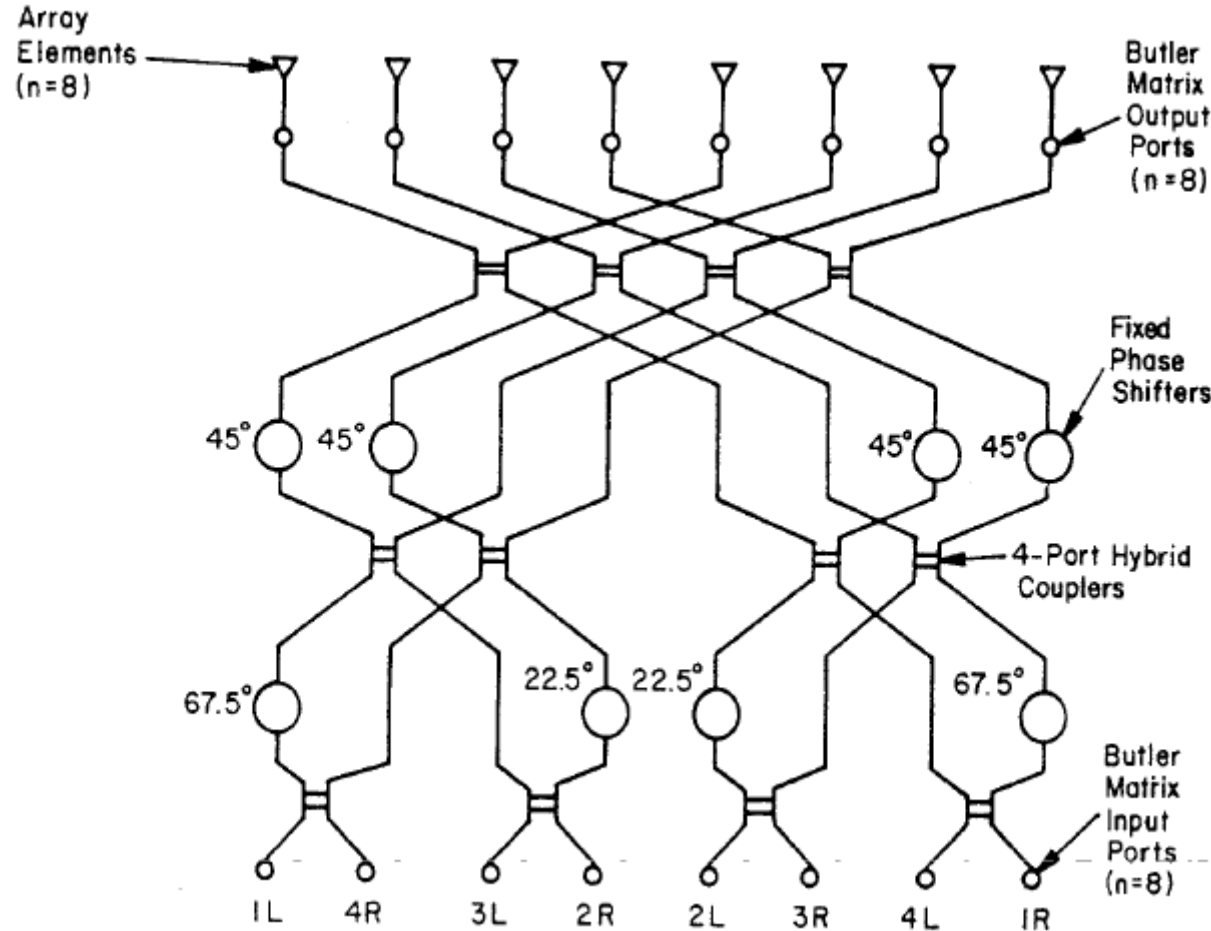
A network of hybrid couplers that implements the DFT – in fact, the hardware equivalent of the Cooley-Tukey FFT algorithm. Principally used to form a set of orthogonal beams from a linear array.



Butler, J. and Lowe, R., 'Beam forming matrix simplifies design of electronically scanned antennas', *Electronic Design*, Vol. 9, April 1961, pp170-173.

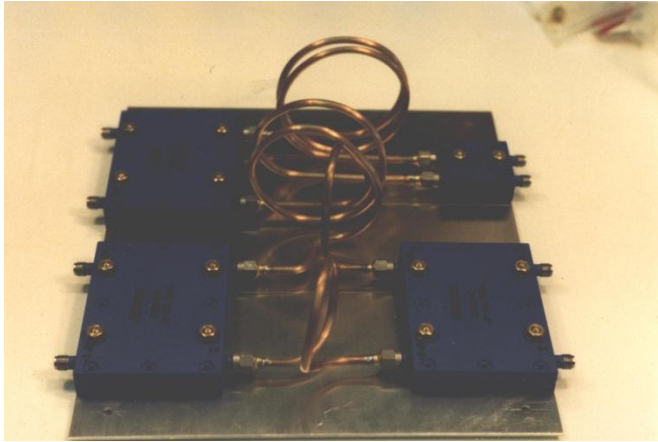
Withers, M.J., 'Frequency-insensitive phase-shift networks and their use in a wide-bandwidth Butler matrix', *Electronics Letters*, Vol. 5, No. 20, pp496-497, October 1969.

# Butler matrix

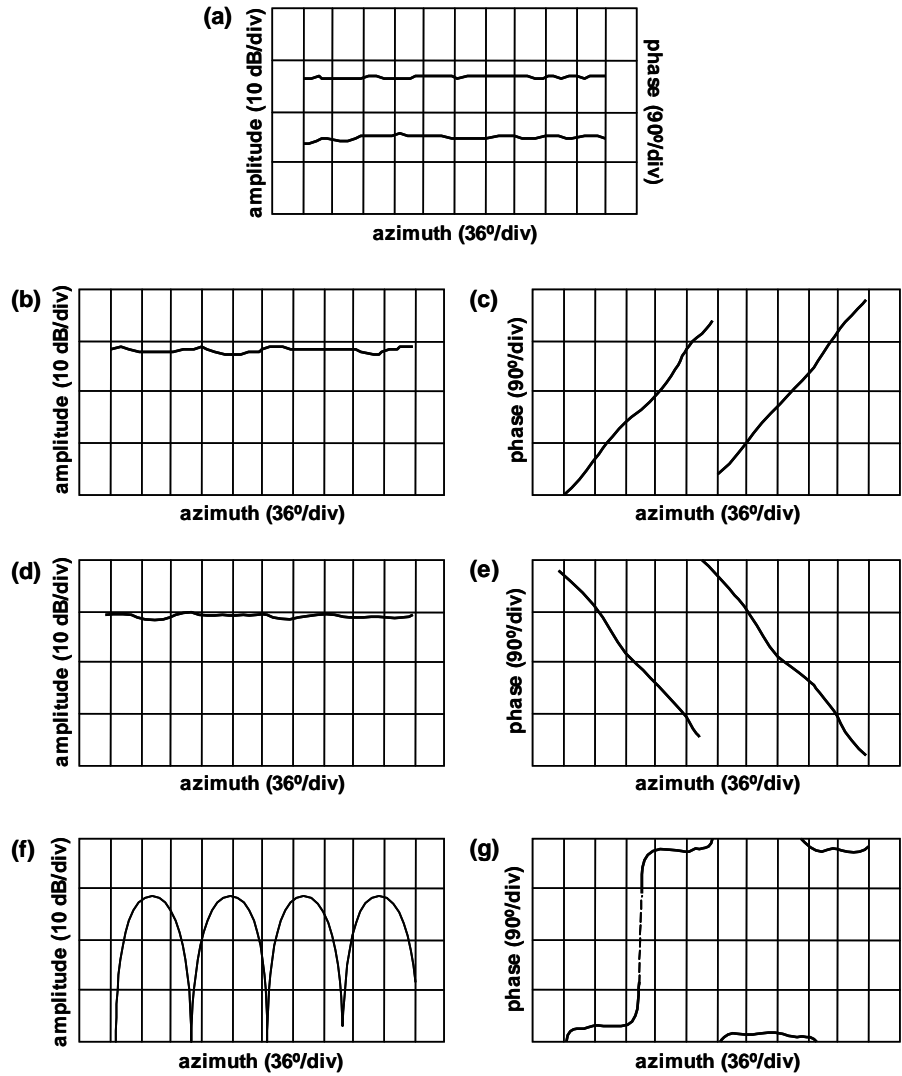


H. Nord, 'Implementation of an 8x8 Butler Matrix in microstrip', Diploma Thesis,  
[http://www.nt.tuwien.ac.at/mobile/theses\\_finished/Master\\_Nord/paper.pdf](http://www.nt.tuwien.ac.at/mobile/theses_finished/Master_Nord/paper.pdf)

# Circular arrays



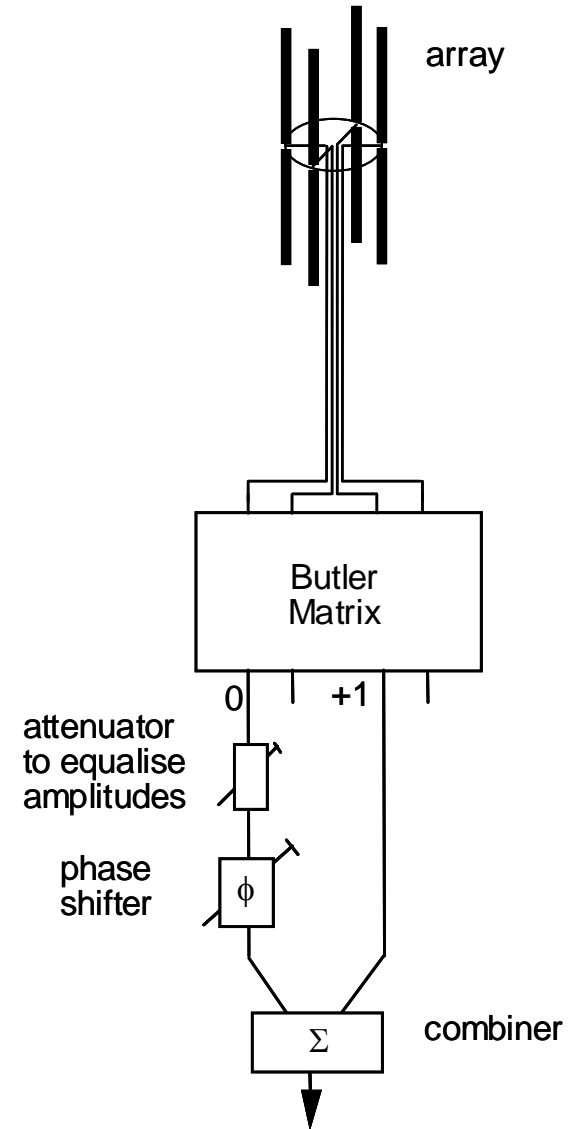
4x4 Butler Matrix



Measured phase mode patterns of a 4-element circular array of monopole elements, at a frequency of 900 MHz, as a function of azimuth angle: (a) zero-order mode amplitude (upper) and phase (lower); (b) +1 order mode amplitude; (c) +1 order mode phase; (d) -1 order mode amplitude; (e) -1 order mode phase; (f) second-order mode amplitude; (g) second-order mode phase. Amplitude: 10 dB/div; phase 90°/div.; horizontal scale (azimuth angle) in each case 36°/div.

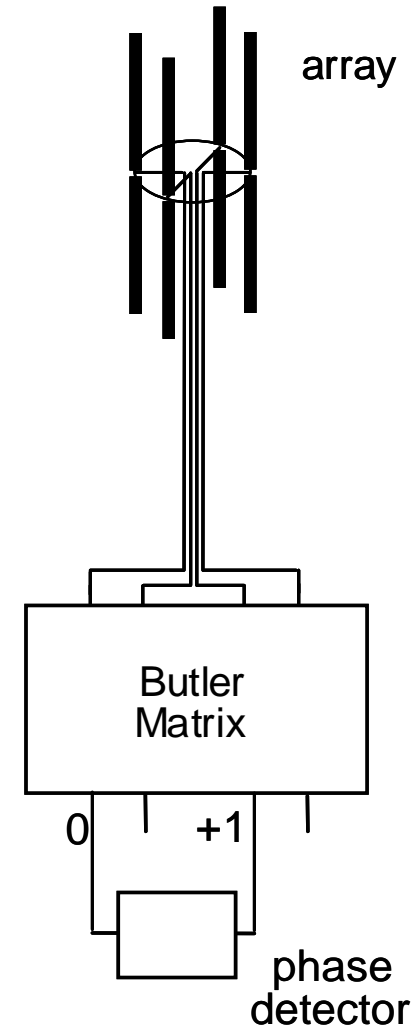
# Null steering

A plane wave incident on the array will excite all phase modes simultaneously. Suppose that the zero-order phase mode and first-order phase mode are equalized in amplitude and added together. It is easy to see that there is one direction in which they will cancel, giving a single null. The direction of this null can be steered by inserting a phase shifter in one of the paths, and the null direction is given directly by the setting of the phase shifter. Furthermore, if the phase mode coefficients  $K_m$  can be characterized and compensated by means of networks with appropriate transfer functions, then the null shape and direction can be maintained over the full instantaneous bandwidth of the array. These results hold for any two phase modes whose orders differ by one.



# DOA measurement

In a rather similar way, if the phase difference is measured between two adjacent phase modes when a plane wave is incident on the array, this phase difference provides a direct reading of the direction of arrival of the signal, and the same comments about broadband operation apply. In fact, if phase modes whose orders differ by two are chosen, then the sensitivity is increased by a factor of two, but at the expense of introducing a  $180^\circ$  ambiguity (which can be resolved by the original measurement). As an example, an experimental system based on this principle has been constructed and demonstrated, operating over the band 2-30 MHz, and has been produced commercially.



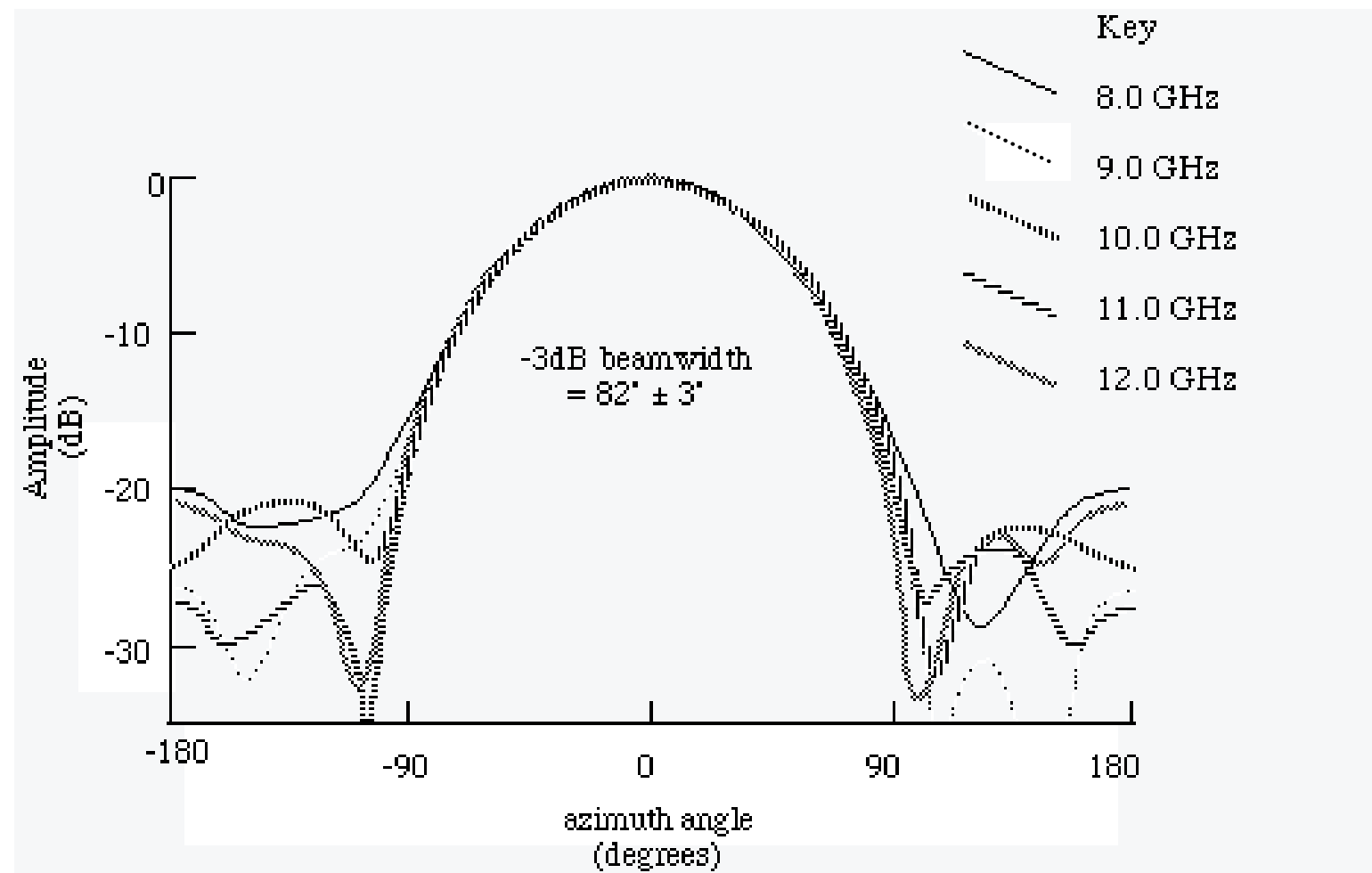
Cvetkovic, M., Davies, D.E.N., Griffiths, H.D. and Collins, B.S., 'An HF direction-finding and null steering system employing a four-element circular array', *Proc. 4th IEE Intl. Conference on HF Radio Systems and Techniques*, London; IEE Conf. Publ. No. 284, pp221-225, April 1988.

# Pattern synthesis

The results quoted for null steering are an example of a much more general application of phase modes to synthesize radiation patterns. Phase modes may be treated in the same way as the elements of a uniformly-spaced linear array, and all the techniques developed for linear array pattern synthesis may be applied to circular arrays, subject to the following comments

- Phase modes are omnidirectional in azimuth, so the ‘elements’ are also omnidirectional. The radiation pattern of the circular array corresponds to the array factor of the linear array.
- Phase modes are orthogonal (since they are the outputs of a discrete Fourier Transform), so there is no mutual coupling.
- The radiation patterns have the same shape (in  $\theta$  space) as those formed by a linear array (in  $kds\sin\theta$  space) with an interelement spacing of  $\lambda/2$ , independent of frequency.
- For a discrete array, exciting a single mode port excites a periodic sequence of modes. For example, if the +1 mode is excited on a four element array, the -7, -3, +5, and +9 modes are also excited. These additional harmonics correspond to additional linear array ‘elements’.

# Circular arrays



Example of instantaneously broadband beam pattern synthesized over the band 8-12 GHz, using a 4-element array of monopoles.

# Isolated omnidirectional patterns

A further property of circular arrays excited by means of phase modes is that there is high isolation between the individual phase mode ports of the Butler Matrix. This arises because of the orthogonality property of the Discrete Fourier Transform.

The phase modes therefore act as isolated omnidirectional patterns, potentially over a broad bandwidth. In practice, imperfections in the Butler Matrix and variations in the impedances presented by the array elements limit the isolation, but it is easy to obtain 20 or 30 dB of isolation without taking any special precautions.

The bandwidth is usually limited by that of the Butler Matrix to an octave or so.

# Sectoral phase modes

Whilst the omnidirectionality property of phase modes is in most cases an attraction, there may be instances where it is a disadvantage, for example in DF applications where there is more than one co-channel signal present. In fact, in the phase-comparison DF scheme, when a 15 dB weaker co-channel signal is also received by the array, the worst-case DOA error is  $2\arcsin 10^{-15/20} = 20.5^\circ$ .

There is therefore some attraction in the ability to form two sets of multibeam patterns, such that each angular sector is covered by a pair of low-sidelobe beams with linear and opposite phase slopes. Amplitude comparison may then be used to unambiguously determine the angular sector facing the incident signal, while a more accurate bearing is obtained by detecting and comparing the phases of the two directional beams covering that sector, just as with ordinary phase modes, but with a much-reduced susceptibility to out-of-sector interference. Such patterns are known as sectoral phase modes.

# Superresolution

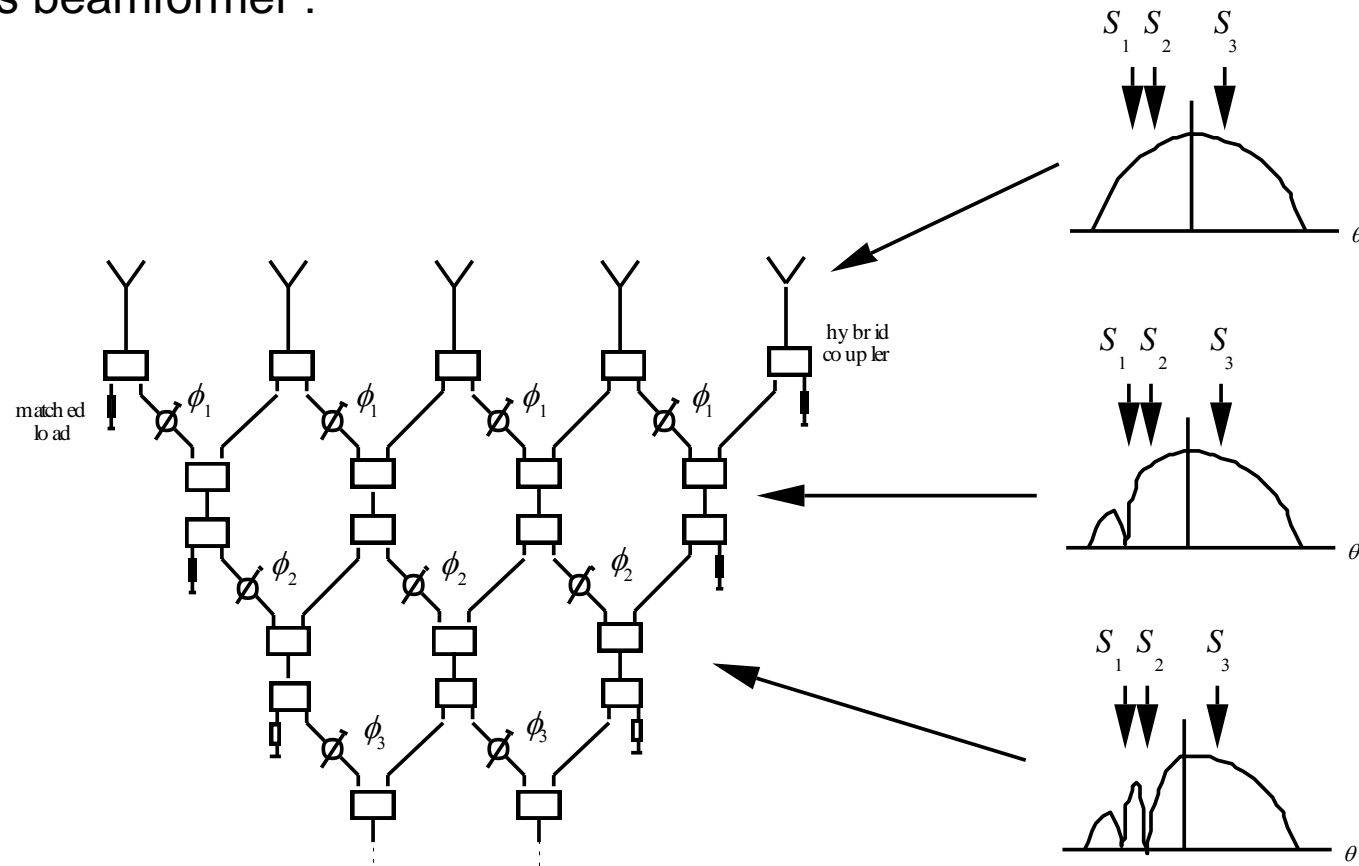
The angular resolution of an antenna system is the ability to resolve the directions of arrival of two signals closely spaced in angle.

Classically, if we form a set of orthogonal beams from an array of length  $D$ , the angular separation between adjacent beams will be  $\lambda/D$  (radians). Thus two signals can be resolved if their angular separation is greater than the angular separation between adjacent beams - in other words, the angular resolution is just  $\lambda/D$ . This is sometimes known as the Rayleigh criterion.

*Superresolution* is a name given to a set of signal processing techniques which achieve better angular resolution than the classical  $\lambda/D$  Rayleigh limit.

# The Davies Beamformer

An intuitive demonstration that this is possible is provided by the 'Davies beamformer'.



# The Davies Beamformer

Suppose there are a set of incident signals  $S_1, S_2, \dots$  incident on a uniformly-spaced linear array at angles  $\theta_1, \theta_2, \dots$  to the array normal. The first signal can be nulled at the outputs of the first set of combiners, by setting all the phase shifters in the first layer to

$$\phi_1 = \frac{2\pi d}{\lambda} \sin \theta_1$$

where  $d$  is the interelement spacing.

The signals at the output of the first layer therefore contain all the signals except  $S_1$ , and the phase shifter settings  $\phi_1$  allow the direction of arrival of  $S_1$  to be determined. In an exactly similar way, the second signal can be nulled at the outputs of the second set of combiners by setting all the phase shifters in the second layer to

$$\phi_2 = \frac{2\pi d}{\lambda} \sin \theta_2$$

and the phase shifter settings  $\phi_2$  allow the direction of arrival of  $S_2$  to be determined.

This procedure can be repeated, nulling each signal at the appropriate layer of the tree. Clearly, then, the directions of arrivals of the signals can be determined, to a precision which can in principle be significantly better than the  $\lambda/D$  Rayleigh limit, and depends in practice on their signal-to-noise ratios,

# The MUSIC algorithm

In 1979, Schmidt presented one of the earliest, and certainly one of the best-known superresolution algorithms, which he named MUltiple Signal Classification (MUSIC).

Consider an  $M$ -element array of arbitrary geometry, with  $n$  incident signals

$$F_1, F_2, \dots, F_n \quad (n \leq M)$$

The element signals  $X_1, X_2, \dots, X_M$  can be written as:

$$X_1 = a_{11}F_1 + a_{21}F_2 + \dots + a_{D1}F_n + W_1$$

$$X_2 = a_{12}F_1 + a_{22}F_2 + \dots + a_{D2}F_n + W_2$$

$$\vdots = \vdots + \vdots + \dots + \vdots + \vdots + \vdots$$

$$X_M = a_{1M}F_1 + a_{2M}F_2 + \dots + a_{DM}F_n + W_M$$

# The MUSIC algorithm

or in matrix notation :

$$\mathbf{X} = \mathbf{AF} + \mathbf{W}$$

Here the terms  $W_1, W_2, \dots, W_M$  represent the noise at the array elements. This noise may be either internally or externally-generated.

The matrix  $\mathbf{A}$  is known as the *array manifold*, and its coefficients depend on the element positions and their directional responses. The  $j^{\text{th}}$  column of  $\mathbf{A}$  is a mode vector  $\mathbf{a}(\theta)$  of responses of the array to the direction of arrival  $\theta_j$ . The mode vectors and  $\mathbf{X}$  can each be visualised as vectors in  $M$ -dimensional space, and  $\mathbf{X}$  is a linear combination of mode vectors, where the coefficients are the elements of  $\mathbf{F}$ .

In fact a similar formulation was published earlier the same year by Bienvenu: Bienvenu, G., 'Influence of the spatial coherence of the background noise on high resolution passive methods', *Proc. IEEE International Conference on Acoustics, Speech and Signal Processing*, Washington DC, IEEE Publication No. 79CH1379-7 ASSP, 2-4 April 199, pp306-309.

# The MUSIC algorithm

The covariance matrix  $\mathbf{R}$  is formed by averaging a number of ‘snapshots’ of the element signals:

$$\begin{aligned}\mathbf{R} &= \overline{\mathbf{XX}^*} \\ &= \mathbf{A}\overline{\mathbf{FF}^*}\mathbf{A}^* + \sigma^2\mathbf{I}\end{aligned}$$

under the assumption that the signals and the noise are uncorrelated, and where the elements of the noise vector  $\mathbf{W}$  are zero mean and of variance  $\sigma^2$ .

# The MUSIC algorithm

The covariance matrix can be broken down into its eigenvectors and eigenvalues

$$\mathbf{R} = \sum_{i=1}^N \lambda_i \mathbf{e}_i \mathbf{e}_i^* = \mathbf{E} \mathbf{L} \mathbf{E}^*$$

The eigenvalues  $\lambda_i$  of the covariance matrix will be

$$\lambda_i > \sigma^2 \text{ for } i = 1, \dots, n, \text{ and } \lambda_i = \sigma^2 \text{ for } i = n+1, \dots, M$$

The number of incident signals can therefore be determined by inspection of the relative magnitudes of the eigenvalues (this information can be plotted as an *eigenvalue spectrum*), or in some situations this information may be known *a priori*.

# The MUSIC algorithm

Consequently, the covariance matrix can be partitioned into an  $n$ -dimensional subspace spanned by the incident signal mode vectors and an  $M-n$  dimensional subspace spanned by the  $M-n$  noise eigenvectors

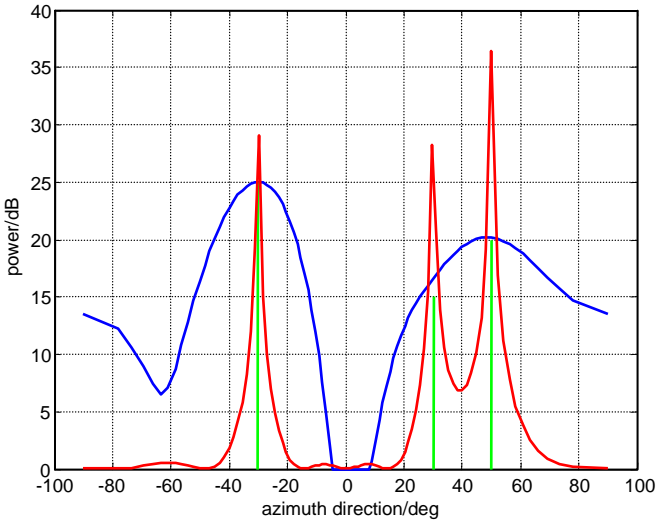
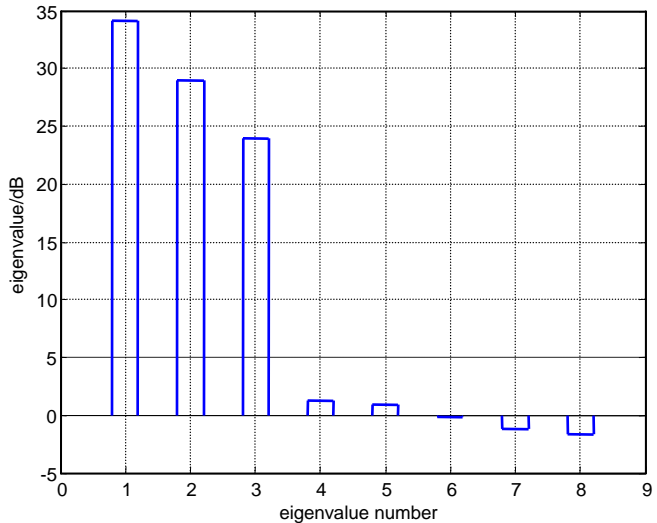
$$\mathbf{R} = \mathbf{E}_s \mathbf{L}_s \mathbf{E}_s^* + \mathbf{E}_N \mathbf{L}_N \mathbf{E}_N^*$$

where  $\mathbf{E}_s$  is the  $M$  by  $n$  signal subspace and  $\mathbf{E}_N$  is the  $M$  by  $M-n$  noise subspace.

The MUSIC algorithm then estimates the angular spectrum  $P(\theta)$  of the incident signals according to

$$P(\theta) = \frac{1}{\mathbf{a}^*(\theta) \mathbf{E}_N \mathbf{E}_N^* \mathbf{a}(\theta)}$$

# The MUSIC algorithm



Simulation of the operation of the MUSIC algorithm with an 8-element linear array, with three signals incident at angles at  $-30^\circ$ ,  $+30^\circ$  and  $+50^\circ$ , at signal-to-noise ratios of 25 dB, 15 dB and 20 dB respectively. The left-hand figure shows the eigenvalue spectrum, from which it can be seen that there are three large eigenvalues corresponding to the three signals, and five smaller ones corresponding to noise level. The right-hand figure plots the MUSIC function. Also shown, for comparison is the response obtained from the conventional beamforming algorithm, using an amplitude taper to lower the sidelobes. The MUSIC algorithm is able to resolve the three signals comfortably, whilst the conventional beamformer algorithm is unable to resolve the two closely spaced signals at all. Results courtesy of David Brandwood, Roke Manor Research.

# Superresolution

Superresolution estimators are usually directly applied to the signals received by the array elements, but it can often be beneficial to preprocess the array outputs by means of a beamforming network, transforming the superresolution scheme from ‘element space’ to ‘beam space’.

Similarly, with circular arrays excited in terms of phase modes, it is possible to operate on the phase mode signals themselves, thereby giving superresolution in ‘phase mode space’. This works because the phase modes can be treated in exactly the same way as the elements of an equispaced linear array, and so any processing technique developed for a linear array can equally be applied to the phase modes of a circular array. This technique has the advantages that the phase modes are omnidirectional, and hence that the same performance is obtained over the full  $360^\circ$  of azimuth, and also that the performance is broadband (over potentially an octave or more).

# Summary

- A bistatic radar can measure bistatic range, Doppler shift or direction of arrival, or any combination of them
- Circular arrays have the advantage that the performance is constant over the full  $360^\circ$  of direction.
- Phase mode processing offers an elegant way of measurement of direction of arrival, of null steering and of pattern synthesis, potentially over a broad bandwidth.
- Superresolution techniques can be used with circular arrays, with the same advantage of  $360^\circ$  coverage and broad bandwidth of operation.

# Further Reading

Griffiths, H.D., 'Circular arrays', in *Modern Antennas* (second edition), Drabowitch, S., Papiernik, A., Griffiths, H.D., Encinas, J. and Smith, B.L., Springer, ISBN 1 4020 3216 1, 2005.

Davies, D.E.N., 'A transformation between the phasing techniques required for linear and circular aerial arrays', *Proc. IEE*, 1965, Vol. 112, No. 11, pp2041-2045.

Rahim, T. and Davies, D.E.N., 'Effect of directional elements on the directional response of circular antenna arrays', *Proc. IEE*, Vol. 129, Pt. H., No. 1, pp18-22, 1982.